Published in final edited form as:
Osteoarthritis Cartilage. 2012 December ; 20(12): 1519–1526. doi:10.1016/j.joca.2012.08.013.

Bone Marrow Lesions are Associated with Altered Trabecular Morphometry

Jeffrey B Driban, PhD, ATC, CSCS[a], **Anna Tassinari**[b], **Grace H Lo, MD, MSc**[c], **Lori Lyn Price, MAS**[d], **Erika Schneider, PhD**[e], **John A Lynch, PhD**[f], **Charles B. Eaton, MD, MS**[g], and **Timothy E. McAlindon, MD, MPH**[h] **for the OAI Investigators Group**

Jeffrey B Driban: jdriban@tuftsmedicalcenter.org; Anna Tassinari: aniat@bu.edu; Grace H Lo: ghlo@bcm.edu; Lori Lyn Price: lprice1@tuftsmedicalcenter.org; Erika Schneider: schneie1@ccf.org; John A Lynch: jlynch@psg.ucsf.edu; Charles B. Eaton: charles_eaton@mhri.org; Timothy E. McAlindon: tmcalindon@tuftsmedicalcenter.org

[a]Division of Rheumatology, Tufts Medical Center, 800 Washington Street, Box #406, Boston, MA 02111

[b]Division of Rheumatology, Tufts Medical Center, 800 Washington Street, Box #406, Boston, MA 02111

[c]Medical Care Line and Research Care Line; Houston Health Services Research and Development (HSR&D) Center of Excellence Michael E. DeBakey VAMC, Houston, TX. Section of Immunology, Allergy, and Rheumatology, Baylor College of Medicine, Houston, TX. 1 Baylor Plaza, BCM-285, Houston, TX 77030

[d]Biostatistics Research Center, Institute for Clinical Research and Health Policy Studies, Tufts Medical Center, 800 Washington Street, Box #63, Boston, MA 02111

Corresponding Author: Jeffrey B. Driban, PhD, ATC, CSCS, Division of Rheumatology, Tufts Medical Center, 800 Washington Street, Box #406, Boston, MA 02111, jdriban@tuftsmedicalcenter.org, Phone: 617-636-7449, Fax: 617-636-1542.

COMPETING INTERESTS

Driban JB– none
Tassinari A – none
Lo GH – none
Price LL – none
Schneider E – none
Lynch JA – none
Eaton CB – none
McAlindon TE – none

AUTHOR CONTRIBUTIONS

Jeffrey B. Driban contributed to the conception and design, analysis and interpretation of data, drafting/revisions of article, as well as final approval of the article.
Anna Tassinari contributed to the conception and design, analysis and interpretation of data, drafting/revisions of article, as well as final approval of the article.
Grace H. Lo contributed to the conception and design, analysis and interpretation of data, drafting/revisions of article, as well as final approval of the article.
Lori Lyn Price contributed to the conception and design, analysis and interpretation of data, drafting/revisions of article, as well as final approval of the article.
Erika Schneider contributed to the analysis and interpretation of data, drafting/revisions of article, as well as final approval of the article.
John A Lynch contributed to the acquisition of data, revisions of article, as well as final approval of the article.
Charles B. Eaton contributed to the acquisition of images, revisions of article, as well as final approval of the article.
Timothy McAlindon contributed to the conception and design, analysis and interpretation of data, drafting/revisions of article, as well as final approval of the article.

[e]Imaging Institute, Cleveland Clinic Foundation, 9500 Euclid Avenue HB6, Cleveland, OH 44195

[f]Department of Epidemiology and Biostatistics, University of California at San Francisco, 185 Berry Street, Lobby 5, Suite 5700, San Francisco, CA 94107

[g]Departments of Family Medicine and Epidemiology, Alpert Medical School of Brown University, Center for Primary Care and Prevention, Second Floor, Memorial Hospital of Rhode Island, 111 Brewster Street, Pawtucket, RI 02864

[h]Division of Rheumatology, Tufts Medical Center, 800 Washington Street, Box #406, Boston, MA 02111

Abstract

Objective—Bone marrow lesions (BMLs) are a common magnetic resonance (MR) feature in patients with osteoarthritis, however their pathological basis remains poorly understood and has not been evaluated *in vivo*. Our aim was to evaluate the trabecular structure associated with the presence and size of BMLs present in the same regions of interest (ROI) using quantitative MR-based trabecular morphometry.

Design—158 participants in the Osteoarthritis Initiative (OAI) were imaged with a coronal 3D FISP sequence for trabecular morphometry in the same session as the OAI 3T MR knee evaluation. The proximal medial tibial subchondral bone in the central weight-bearing ROI on these knee 3D FISP images were quantitatively evaluated for apparent bone volume fraction, trabecular number, spacing, and thickness. BMLs were also evaluated in the subchondral bone immediately adjacent to the articular cartilage. BML volume was also evaluated within the same trabecular morphometry ROI and semi-quantitatively classified as none, small, or large. Kruskal-Wallis test was used to determine if mean apparent bone volume fraction, trabecular number, spacing, or thickness differed by BML score.

Results—Compared to knees with ROIs containing no BMLs, knees with small or large BMLs had statistically higher apparent bone volume fraction ($p<0.01$), trabecular number ($p<0.01$), and thickness ($p=0.02$), and lower trabecular spacing ($p<0.01$).

Conclusions—Compared to knees with ROIs containing no BMLs, knees with ROIs containing small or large BMLs had higher apparent bone volume fraction, trabecular number and thickness, but lower trabecular spacing. These findings may represent areas of locally increased bone remodeling or compression.

Keywords

magnetic resonance imaging; osteoarthritis; knee

INTRODUCTION

Knee osteoarthritis (OA) is a leading cause of disability among Americans[1] and is characterized by multi-tissue (*e.g.,* cartilage, bone) failure of a synovial joint. Processes in the peri-articular bone (*e.g.,* subchondral bone attrition, trabecular remodeling, osteophyte formation, bone marrow lesions [BMLs]) appear to be an integral part of knee OA progression[2–5]. Furthermore, BMLs have also been associated with knee symptoms such as pain and stiffness[3, 6–8].

BMLs are common subchondral trabecular bone features in the OA population and are identified as epiphyseal marrow regions with high-signal intensity on fat-suppressed intermediate-weighted (IW) or fat-suppressed T2-weighted spin echo (SE) or turbo spin echo (TSE) magnetic resonance (MR) images[9–13]. BMLs may be clinically significant

because they have been found to relate to knee OA symptoms and structural progression[3, 6–8, 11, 14–20]. While BMLs are known to represent structural changes in the bone[12, 13, 21–23], histomorphological studies have only evaluated knees with end-stage OA prior to arthroplasty or excised tissue samples[12, 13, 21–23]. These studies suggest that BMLs are characterized by bone marrow necrosis, fibrovascular tissue growth, reduced mineral density, and abnormal trabeculae[12, 13, 21–23].

High-resolution MR imaging (Figure 1a,b) permits *in-vivo* measurement of trabecular morphology, including apparent bone volume fraction (aBV/TV), trabecular number (aTb.N), trabecular spacing (aTb.Sp), and trabecular thickness (aTb.Th) [24–28]. In this cross-sectional study, our goal was to study bone morphological features in subchondral trabecular regions with and without BMLs using high-resolution MR images. We hypothesized that BMLs represent areas of local bone remodeling and that their presence should therefore relate to higher aBV/TV, aTb.N, and aTb.Th, but lower aTb.Sp.

METHOD

Study sample

This was a cross-sectional analysis of a convenience sample from the Bone Ancillary Study (1R01AR054938) of the Osteoarthritis Initiative (OAI). The OAI is a multi-center observational study of knee OA that is collecting longitudinal clinical and image data over a nine year period. The primary aim of the Bone Ancillary Study was to investigate the influence of bone in the structural progression of OA. The present study is a secondary analysis of the Bone Ancillary Study.

The Bone Ancillary Study recruited participants from the OAI progression subcohort. To be a member of the OAI progression subcohort each participant had at least one knee with radiographic OA (Osteoarthritis Research Society International [OARSI] atlas osteophyte grade 1 to 3)[29] determined from bilateral fixed-flexion radiographs as well as frequent symptoms (“pain, aching or stiffness on most days of the month in the last year”); both were assessed at the OAI baseline visit. Additional information regarding the inclusion and exclusion criteria for the OAI progression subcohort is available at http://oai.epi-ucsf.org.

Bone Ancillary Study participants were recruited at the OAI 30- or 36-month visit from the progression subcohort at which time they had the core OAI MR acquisitions as well as a high-resolution, trabecular morphometry sequence performed on the primary OAI knee (usually the right knee) at the same visit. Participants presented here are from the first half of the Bone Ancillary Study; these participants were recruited and imaged between August 2007 and March 2009.

MR Imaging

A coronal-oblique 3D fast imaging with steady state precession (FISP) sequence (Figure 1a,b)[24] was obtained on the primary OAI knee using one of four identical Siemens Trio 3T MR systems and a USA Instruments quadrature transmit-receive knee coil at one of four OAI clinical sites. The primary OAI knee was usually the right knee unless there was a contraindication (*e.g.,* presence of metal), in which case, the left knee was identified as the primary OAI knee. Selection of the primary OAI knee was advantageous because the complete set of OAI MR acquisitions were performed on this knee, whereas the contralateral knee had an abbreviated MR acquisition to reduce participant burden. Therefore, the primary OAI knee was not always the knee with symptomatic radiographic OA.

These coronal double-oblique 3D FISP images[24] were used to visualize the subchondral trabecular bone and were obtained in 10.5 minutes using 72 slices, 1 mm slice thickness,

0.23 mm × 0.23 mm in-plane spatial resolution, 12 cm field of view (FOV), 512 × 512 matrix (interpolated to 1024 × 1024), 4.92 ms echo time (TE) (fat-water in-phase), 20 ms recovery time (TR), 50° flip angle, 180 Hz/pixel readout bandwidth, and phase encode right/left. The chemical shift artifact is 2.4 pixels shifted superior, outside the femoral subchondral bone.

The image contrast of a FISP acquisition is determined by the T2*/T1 ratio of the tissue, and is mostly dependent on the TR and flip angle. With the above acquisition parameters, joint fluid ranges from 20% less to 33% higher signal intensity than "normal" tibial epiphyseal marrow (defined as areas without MR evidence of BMLs, sclerosis, fracture, cysts, or other abnormalities), whereas signal levels inside BMLs are much lower and are often half that of marrow. In other words, signal intensity inside BMLs is lower than that of the joint fluid. The joint fluid signal intensity is location dependent due to the radiofrequency transmit uniformity of the knee coil[30]. In this image set, when mid-joint, the joint fluid has approximately 20% lower signal than the marrow. Because the fat and water protons are in-phase at 4.9 ms TE at 3T, the fat and water signal is additive and the resultant image lends itself to automated analysis using the single threshold approach described in Newitt *et al*[31]. Assessments in the regions of BMLs, however, should be approached carefully because the lower fluid signal levels that occur in regions with BMLs can cause a systematic overestimation of bone in these regions due to partial volume effects. We attempted to minimize the impact of partial volume artifacts, by selecting the signal value of cortical bone as our threshold.

From the core OAI knee MR protocol[10] that was acquired in the same exam session and on the same knee as the coronal 3D FISP trabecular sequence, the sagittal fat-suppressed intermediate-weighted (IW) TSE series (Figure 2a) were used to score BML presence and extent[3, 9, 10, 12, 32]. The IW FS TSE images were obtained using 3 mm slice thickness, 0.36 mm × 0.51 mm in-plane spatial resolution, 16 cm FOV, 313 × 448 matrix (interpolated to 512 × 512), 30 ms TE, 3200 ms TR, and phase encode superior/inferior. In addition, the coronal non-fat suppressed IW TSE series (Figures 1c, d) was used as an orthogonal reference system to help determine extent of the ROI and BML in the coronal plane. The coronal IW TSE images were obtained using 3 mm slice thickness, 0.37 mm × 0.46 mm in-plane spatial resolution, 14 cm FOV, 307 × 384 matrix (interpolated to 512 × 512), 29 ms TE, 3850 ms TR, and phase encode right/left.

Quality assessments of the MR images were performed for contrast, field-of-view (FOV) placement, and absence of motion artifacts. The MR systems underwent the standard OAI quality control protocol[30].

MR Image Analysis

The coronal 3D FISP images were quantitatively analyzed using CalcDCN software; this analysis tool was developed and validated at the University of California, San Francisco[31, 33–40]. Briefly, the images were analyzed as follows. First, a standardized signal intensity threshold was applied to the images to create a bone mask[31]. The signal threshold was chosen based on the cortical bone signal intensity from twenty circular 0.7 mm diameter ROI in the medial and lateral femoral condyles. Next, a rectangular ROI was placed on the 20 consecutive central MR imaging slices[41] in the proximal medial tibial epiphyseal subchondral bone, immediately below the cartilage (Figure 1a). To improve the reliability of the trabecular morphometry measures the ROI included the subchondral cortical bone plate. The medial tibiofemoral compartment was selected for this analysis as it has a higher prevalence of OA[42] and BMLs[43] compared to the lateral compartment and is exposed to greater compressive loading[44, 45]. The ROI had a constant height of 3.75 mm. A single reader (AT) placed an ROI with a width of 15.0 mm and then adjusted the ROI width

between 13.5 and 17.0 mm (n = 50, 31.6% ROI widths were adjusted), depending on the size of the medial tibial plateau. Apparent trabecular morphometry (*i.e.,* aBV/TV, aTb.N, aTb.Sp, and aTb.Th) were calculated as previously reported[39] for each ROI in each slice, and averaged across the 20 slices. In brief, aBV/TV represents the ratio of the number of pixels contributing to the trabecular bone signal to the total number of pixels within the ROI. Apparent trabecular thickness (aTb.Th) is the average of the mean intercept length for all angles of parallel rays passing through a given image and intersecting boundaries between bone and marrow. Apparent trabecular number (aTb.N) is the ratio between the area fraction of bone and aTb.Th. Finally, aTb.Sp is derived from the equation (1 / aTb.N)-aTb.Th. Intra-rater (test-retest) reliability was excellent with an intraclass-correlation coefficient of 0.99 (n=12, assessed at least 3 days apart). One analyst performed all the quantitative measurements.

BMLs were defined as areas of increased signal intensity in the bone marrow, visible on at least two consecutive slices on the sagittal IW fat-suppressed TSE sequence, and located in the subchondral bone immediately adjacent to the articular cartilage and below the cortical bone in the proximal medial tibial epiphysis[46, 47]. BMLs were assigned to one of three categories based on the estimated volume of the BML within the trabecular ROI: 1) “none”, if no BML was present within the ROI; 2) “small”, if the BML comprised 1–49% of the ROI; and 3) “large”, if the BML comprised at least 50% of the ROI. To estimate the percentage of the ROI occupied by a BML, the coronal 3D FISP trabecular images (Figures 1a,b) were manually registered with the coronal IW TSE images (Figures 1c,d). The coronal IW TSE images were used as an orthogonal reference to help localize the ROI and the BML visualized on the fat-suppressed sagittal IW TSE images (*e.g.,* sagittal image 1a corresponds to the coronal image 1c and sagittal image 1b corresponds to coronal image 1d). The range of sagittal slices (Figure 2a) that the BMLs spanned was determined by counting the number of sagittal slices within the ROI using the eFilm 3D Cursor tool (MERGE Healthcare, Chicago, IL). Furthermore, the reader used the eFilm 3D Cursor tool to determine the anterior and posterior borders of the ROI on the sagittal slices (see Figure 2a). All BML assessments were performed by one analyst (AT) at a separate session than when trabecular morphometry assessments were made.

Semi-quantitative Knee OA Assessments

Centralized semi-quantitative assessments of radiographic knee OA severity[48] were performed using the weight-bearing posterior-anterior fixed-flexion knee radiographs collected at the 24-month OAI visit. Kellgren-Lawrence grades (0 to 4) as well as a modified OARSI-atlas based joint space narrowing (JSN) scores[29] were obtained from the public data release (kxr_sq_bu, release version 3.1).

Statistical Analysis

Descriptive characteristics (*e.g.,* ethnicity, body mass index) were calculated. The distribution of radiographic knee OA severity was based on the centrally scored 24-month KL grade and medial JSN scores. The absence of medial JSN was defined as a JSN equal to zero. Since the data were skewed (skewness range = 0.32 to 3.33, kurtosis range = −0.43 to 15.06), we used the natural log of the trabecular morphometry measures to perform four analyses of variance (ANOVAs) to evaluate whether mean aBV/TV, aTb.N, aTb.Sp, and aTb.Th differed by BML score. However, the model assumptions were not met due to the data not being normally distributed (skewness range = −1.05 to 1.30, kurtosis range = 0.71 to 2.77), even after taking the log; therefore, we used the nonparametric Kruskal-Wallis tests to evaluate if there were differences between groups. If the p-value for the overall Kruskal-Wallis test was statistically significant ($p<0.05$), then we examined all pair-wise comparisons. We also used robust regression models with trabecular morphometry measures

as the outcomes to determine if the association between BML score and trabecular metric outcomes held after adjusting for potential confounders, including age, gender, ethnicity, and BMI. All analyses were performed using SAS 9.2 (Cary, North Carolina, USA).

RESULTS

The 158 subjects included in this analysis were 51.9% female, 13.3% Black, 3.2% Hispanic, and had a mean ± standard deviation age of 69.0 ± 8.9 years, and mean body mass index of 29.2 ± 5.0 kg/m^2. There were 149 right knees and 9 left knees with a Kellgren - Lawrence grade distribution from 0 to 4 of 13%, 15%, 33%, 29%, and 10%, respectively. The majority of participants had no BMLs contained within the subchondral trabecular ROI: 78.5% had no BMLs, 15.2% had a small BML, and 6.3% had a large BML. Thirty-three participants were missing centrally-scored medial JSN (27 with no BMLs, 4 with small BMLs, and 2 with large BMLs). Among participants with no medial JSN (JSN score=0; n=61), 97% had no BMLs, 3% had small BMLs, and 0% had large BMLs. In contrast, a larger percent of participants with medial JSN (n=64) had BMLs within the ROI: 59% had no BMLs, 28% had small BMLs, and 6% had large BMLs.

The four Kruskal-Wallis tests evaluating trabecular morphometry metrics were statistically significant, suggestive of differences among those with different BML sizes (Table 1, Figure 3). Compared to ROIs without BMLs, ROIs with BMLs had higher aBV/TV (small: p=0.0009; large: p= 0.002), aTb.N (small: p=0.005; large: p=0.004), and aTb.Th (small: p<0.0001; large: p=0.002). ROIs with BMLs had lower aTb.Sp compared to ROIs without BMLs (small: p=0.006; large: p=0.0.03). The associations remained statistically significant even after adjusting for potential confounders (*i.e.,* age, gender, ethnicity, and BMI). Differences in morphometry metrics between the small and large BML groups did not reach statistical significance: aBV/TV (p=0.34), aTb.N (p=0.30), aTb.Sp (p=0.84), and aTb.Th (p=0.50).

DISCUSSION

Using *in-vivo* MR-based apparent trabecular morphometry metrics we found that medial tibial trabecular characteristics of aBV/TV, aTb.N, aTb.Th, and aTb.Sp are statistically different in the presence of a BML. This means regions with BMLs are characterized by trabeculae that are thickened, increased in number, and with less spacing. These quantitative findings are in agreement with subjectively observed differences in the subchondral trabecular bone on MR and radiography including sclerosis[29]. The observed differences are compatible with the hypotheses that BMLs may represent localized regions of trabecular remodeling or compression.

The present findings concur with previous analyses of the trabecular structure within BMLs (i.e., increased bone volume fraction and trabecular thickness)[21]. In contrast to previous findings, the current measurements detected a statistically significant difference in aTb.N and aTb.Sp. The disparity in trabecular number and spacing findings may be related to the differences in how the tissues were measured (*e.g., in vivo* versus excised bone samples), imaging modality (MR observes bone indirectly through changes in the marrow signal, computed tomography [CT] observes bone directly), spatial resolution, or sample size. Micro-CT with excised bone samples and *in vivo* human peripheral CT scans can detect smaller trabecular structures (e.g., spatial resolution of > 1 microns and 130 microns; respectively)[21, 49] than high-resolution *in-vivo* MR imaging (spatial resolution: 200 microns × 200 microns × 1000 microns)[24]. Though MR imaging lacks sensitivity to these smaller trabecular structures, it may be able to focus on differences in the larger scale structures. Furthermore, MR images can be obtained with minimal risk to living participants, which

facilitated our ability to measure trabecular characteristics on a large number of knees. The previous published study[21] only included only 6 patients, which may have limited their ability to detect change in trabecular number; in contrast, 158 knees were included in the current study.

A limitation of this study is that the ROIs were located only in the central medial tibial subchondral bone and included the subchondral cortical bone plate. The results of this work cannot be generalized to trabecular morphology differences in other regions of the knee joint or determine if the the association between BMLs and trabecular morphology changes in different regions of the knee. However, we focused on this region because tibiofemoral OA most frequently involves the medial compartment[42]. This region could be influenced by sclerotic changes in addition to BMLs but further research is necessary to assess the relationship between sclerotic changes in and near BMLs[21]. Another limitation is that we systematically used a small rectangular ROI independent of the size and shape of BMLs present within a knee. This could possibly lead to misclassification of the BMLs, as some large BMLs may be categorized as "small" due to the small fraction of ROI they occupy. Future studies may help clarify whether large BMLs near the trabecular ROI influence trabecular structure. However, since the ROI was predetermined it may be optimal to evaluate the association between BMLs and trabecular structure using a BML score relative to the ROI size. The ROI size varied between 13.5 mm and 17 mm which could influence the BML scores; however, there were only 10 large BMLs thus minimizing the risk of misclassifying BMLs.

Another limitation is that we used a single threshold in the area around a BML. This could potentially introduce a systematic bias toward increased bone volume fraction in spite of the use of a conservative threshold value taken from cortical bone. The impact of this limitation may be reduced in a longitudinal study[50]. Alternative analysis approaches are under development and validation[50]. The cross-sectional nature of this study constitutes another limitation. BML presence and size can fluctuate over time[51] but it is unclear if and how trabecular morphometry changes in relation to BMLs or if the timescales / order of change are the same. Longitudinal evaluations are needed to determine how changes in BMLs size and presence relate to trabecular quantitative metrics and how both relate to OA progression.

Another limitation to our study is that trabecular MR imaging provides an indirect assessment of bone since the proton signal emanating from the marrow provides a high intensity signal whereas cortical and trabecular bone have no visible proton signal using human *in-vivo* MR systems. Therefore, the trabecular measures are an assessment of the areas without high signal, and thus are an indirect or *apparent* measure of trabecular morphometry. Although an important limitation, the fact that these images can be obtained *in vivo* allows for the conduct of longitudinal studies and enhanced ability to include knees with little or mild disease in studies that are both cross-sectional and longitudinal in nature.

Using non-invasive *in-vivo* MR imaging of knees with a range of radiographic OA, we quantified apparent trabecular morphologic metrics in the load-bearing tibial plateau. We found greater apparent bone volume, trabecular number, and trabecular thickness in regions with any BML size. A strength of our study is the inclusion of normal and mild radiographic OA knees; however, this limited the number of knees with BMLs (22% of knees in this cohort). The low prevalence of BMLs is in agreement with previous research that indicated only 10 to 40% of knees with no to moderate knee OA (Kellgren-Lawrence grades 0 to 2) have BMLs (regardless of region)[35, 52]. The small number of knees with BMLs in the central medial tibia likely limited our ability to detect statistically significant differences in quantitative trabecular differences in ROIs with small and large BMLs as well as prevented more complex modeling to control for intra- articular lesions (*e.g.*, meniscal pathology) or

stratified analyses (*e.g.*, knees with or without medial JSN, knees with or without meniscal pathology or other intra-articular lesions).

These data suggest that there are statistically significant differences in the trabecular morphology in regions of subchondral bone with BMLs compared to regions without BMLs. The differences may indicate that areas of subchondral bone containing a BML are local regions of trabecular remodeling or compression. Longitudinal studies may help determine the causal relationships between trabecular morphometry and BMLs.

Acknowledgments

The authors would like to acknowledge Dr. Sharmila Majumdar (University of California, San Francisco) for her advice and for providing CalcDCN, a program for quantifying trabecular morphometry.

This work was supported in part by the Houston VA HSR&D Center of Excellence (HFP90-020). The views expressed in this article are those of the author(s) and do not necessarily represent the views of the Department of Veterans Affairs.

ROLE OF FUNDING SOURCE

The Role of Bone in Knee Osteoarthritis Progression is supported by NIH/NIAMS (grant 1R01AR054938). The OAI is a public-private partnership comprised of five contracts (N01-AR-2-2258; N01-AR-2-2259; N01-AR-2-2260; N01-AR-2-2261; N01-AR-2-2262) funded by the National Institutes of Health, a branch of the Department of Health and Human Services, and conducted by the OAI Study Investigators. Private funding partners include Merck Research Laboratories; Novartis Pharmaceuticals Corporation, GlaxoSmithKline; and Pfizer, Inc. Private sector funding for the OAI is managed by the Foundation for the National Institutes of Health. This manuscript was prepared using an OAI public use data set and does not necessarily reflect the opinions or views of the OAI investigators, the NIH, or the private funding partners. The views expressed in this article are those of the author(s) and do not necessarily represent the views of the Department of Veterans Affairs.

References

1. Guccione AA, Felson DT, Anderson JJ, Anthony JM, Zhang Y, Wilson PW, et al. The effects of specific medical conditions on the functional limitations of elders in the Framingham Study. American Journal of Public Health. 1994; 84:351–8. [PubMed: 8129049]
2. Neogi T, Felson D, Niu J, Lynch J, Nevitt M, Guermazi A, et al. Cartilage loss occurs in the same subregions as subchondral bone attrition: a within-knee subregion-matched approach from the Multicenter Osteoarthritis Study. Arthritis and Rheumatism. 2009; 61:1539–44. [PubMed: 19877101]
3. Hunter DJ, Lo GH, Gale D, Grainger AJ, Guermazi A, Conaghan PG. The reliability of a new scoring system for knee osteoarthritis MRI and the validity of bone marrow lesion assessment: BLOKS (Boston Leeds Osteoarthritis Knee Score). Annals of the Rheumatic Diseases. 2008; 67:206–11. [PubMed: 17472995]
4. Kraus VB, Feng S, Wang S, White S, Ainslie M, Brett A, et al. Trabecular morphometry by fractal signature analysis is a novel marker of osteoarthritis progression. Arthritis and Rheumatism. 2009; 60:3711–22. [PubMed: 19950282]
5. Goldring, SR. Role of bone in osteoarthritis pathogenesis. Vol. 93. Medical Clinics of North America; 2009. p. 25-35.p. xv
6. Yusuf E, Kortekaas MC, Watt I, Huizinga TW, Kloppenburg M. Do knee abnormalities visualised on MRI explain knee pain in knee osteoarthritis? A systematic review. Annals of the Rheumatic Diseases. 2011; 70:60–67. [PubMed: 20829200]
7. Torres L, Dunlop DD, Peterfy C, Guermazi A, Prasad P, Hayes KW, et al. The relationship between specific tissue lesions and pain severity in persons with knee osteoarthritis. Osteoarthritis and Cartilage. 2006; 14:1033–40. [PubMed: 16713310]
8. Lo GH, McAlindon TE, Niu J, Zhang Y, Beals C, Dabrowski C, et al. Bone marrow lesions and joint effusion are strongly and independently associated with weight-bearing pain in knee

osteoarthritis: data from the osteoarthritis initiative. Osteoarthritis and Cartilage. 2009; 17:1562–69. [PubMed: 19583959]

9. Peterfy CG, Gold G, Eckstein F, Cicuttini F, Dardzinski B, Stevens R. MRI protocols for whole-organ assessment of the knee in osteoarthritis. Osteoarthritis and Cartilage. 2006; 14 (Suppl A):A95–111. [PubMed: 16750915]
10. Peterfy CG, Schneider E, Nevitt M. The osteoarthritis initiative: report on the design rationale for the magnetic resonance imaging protocol for the knee. Osteoarthritis and Cartilage. 2008; 16:1433–41. [PubMed: 18786841]
11. Sowers MF, Hayes C, Jamadar D, Capul D, Lachance L, Jannausch M, et al. Magnetic resonance-detected subchondral bone marrow and cartilage defect characteristics associated with pain and X-ray-defined knee osteoarthritis. Osteoarthritis and Cartilage. 2003; 11:387–93. [PubMed: 12801478]
12. Zanetti M, Bruder E, Romero J, Hodler J. Bone marrow edema pattern in osteoarthritic knees: correlation between MR imaging and histologic findings. Radiology. 2000; 215:835–40. [PubMed: 10831707]
13. Saadat E, Jobke B, Chu B, Lu Y, Cheng J, Li X, et al. Diagnostic performance of in vivo 3-T MRI for articular cartilage abnormalities in human osteoarthritic knees using histology as standard of reference. European Radiology. 2008; 18:2292–302. [PubMed: 18491096]
14. Davies-Tuck M, Wluka AE, Forbes A, Wang Y, English DR, Giles GG, et al. Development of bone marrow lesions is associated with adverse effects on knee cartilage while resolution is associated with improvement - a potential target for prevention of knee osteoarthritis: a longitudinal study. Arthritis Research & Therapy. 2010; 19(12):R10. [PubMed: 20085624]
15. Hernandez-Molina G, Guermazi A, Niu J, Gale D, Goggins J, Amin S, et al. Central bone marrow lesions in symptomatic knee osteoarthritis and their relationship to anterior cruciate ligament tears and cartilage loss. Arthritis and Rheumatism. 2008; 58:130–36. [PubMed: 18163483]
16. Kothari A, Guermazi A, Chmiel JS, Dunlop D, Song J, Almagor O, et al. Within-subregion relationship between bone marrow lesions and subsequent cartilage loss in knee osteoarthritis. Arthritis Care and Research. 2010; 62:198–203. [PubMed: 20191518]
17. Raynauld JP, Martel-Pelletier J, Berthiaume MJ, Abram F, Choquette D, Haraoui B, et al. Correlation between bone lesion changes and cartilage volume loss in patients with osteoarthritis of the knee as assessed by quantitative magnetic resonance imaging over a 24-month period. Annals of the Rheumatic Diseases. 2008; 67:683–88. [PubMed: 17728333]
18. Roemer FW, Guermazi A, Javaid MK, Lynch JA, Niu J, Zhang Y, et al. Change in MRI-detected subchondral bone marrow lesions is associated with cartilage loss: the MOST Study. A longitudinal multicentre study of knee osteoarthritis. Annals of the Rheumatic Diseases. 2009; 68:1461–65. [PubMed: 18829615]
19. Roemer FW, Neogi T, Nevitt MC, Felson DT, Zhu Y, Zhang Y, et al. Subchondral bone marrow lesions are highly associated with, and predict subchondral bone attrition longitudinally: the MOST study. Osteoarthritis and Cartilage. 2010; 18:47–53. [PubMed: 19769930]
20. Tanamas SK, Wluka AE, Pelletier JP, Pelletier JM, Abram F, Berry PA, et al. Bone marrow lesions in people with knee osteoarthritis predict progression of disease and joint replacement: a longitudinal study. Rheumatology. 2010; 49:2413–19. [PubMed: 20823092]
21. Hunter DJ, Gerstenfeld L, Bishop G, Davis AD, Mason ZD, Einhorn TA, et al. Bone marrow lesions from osteoarthritis knees are characterized by sclerotic bone that is less well mineralized. Arthritis Research & Therapy. 2009; 11:R11. [PubMed: 19171047]
22. Leydet-Quilici H, Le CT, Bouvier C, Giorgi R, Argenson JN, Champsaur P, et al. Advanced hip osteoarthritis: magnetic resonance imaging aspects and histopathology correlations. Osteoarthritis and Cartilage. 2010; 18:1429–35. [PubMed: 20727415]
23. Bergman AG, Willen HK, Lindstrand AL, Pettersson HT. Osteoarthritis of the knee: correlation of subchondral MR signal abnormalities with histopathologic and radiographic features. Skeletal Radiology. 1994; 23:445–48. [PubMed: 7992110]
24. Schneider E, Lo GH, Sloane G, Fanella L, Hunter DJ, Eaton CB, et al. Magnetic resonance imaging evaluation of weight-bearing subchondral trabecular bone in the knee. Skeletal Radiology. 2011; 40:95–103. [PubMed: 20449585]

25. Lancianese SL, Kwok E, Beck CA, Lerner AL. Predicting regional variations in trabecular bone mechanical properties within the human proximal tibia using MR imaging. Bone. 2008; 43:1039–46. [PubMed: 18755303]
26. Bolbos RI, Zuo J, Banerjee S, Link TM, Ma CB, Li X, et al. Relationship between trabecular bone structure and articular cartilage morphology and relaxation times in early OA of the knee joint using parallel MRI at 3 T. Osteoarthritis and Cartilage. 2008; 16:1150–9. [PubMed: 18387828]
27. Beuf O, Ghosh S, Newitt DC, Link TM, Steinbach L, Ries M, et al. Magnetic resonance imaging of normal and osteoarthritic trabecular bone structure in the human knee. Arthritis and Rheumatism. 2002; 46:385–93. [PubMed: 11840441]
28. Lindsey CT, Narasimhan A, Adolfo JM, Jin H, Steinbach LS, Link T, et al. Magnetic resonance evaluation of the interrelationship between articular cartilage and trabecular bone of the osteoarthritic knee. Osteoarthritis and Cartilage. 2004; 12:86–96. [PubMed: 14723868]
29. Altman RD, Gold GE. Atlas of individual radiographic features in osteoarthritis, revised. Osteoarthritis and Cartilage. 2007; 15 (Suppl A):A1–56. [PubMed: 17320422]
30. Schneider E, NessAiver M, White D, Purdy D, Martin L, Fanella L, et al. The osteoarthritis initiative (OAI) magnetic resonance imaging quality assurance methods and results. Osteoarthritis and Cartilage. 2008; 16:994–1004. [PubMed: 18424108]
31. Newitt DC, van Rietbergen B, Majumdar S. Processing and analysis of in vivo high-resolution MR images of trabecular bone for longitudinal studies: reproducibility of structural measures and micro-finite element analysis derived mechanical properties. Osteoporosis International. 2002; 13:278–87. [PubMed: 12030542]
32. Peterfy CG, Guermazi A, Zaim S, Tirman PF, Miaux Y, White D, et al. Whole-Organ Magnetic Resonance Imaging Score (WORMS) of the knee in osteoarthritis. Osteoarthritis and Cartilage. 2004; 12:177–90. [PubMed: 14972335]
33. Beuf O, Ghosh S, Newitt DC, Link TM, Steinbach L, Ries M, et al. Magnetic resonance imaging of normal and osteoarthritic trabecular bone structure in the human knee. Arthritis Rheum. 2002; 46:385–93. [PubMed: 11840441]
34. Blumenkrantz G, Lindsey CT, Dunn TC, Jin H, Ries MD, Link TM, et al. A pilot, two-year longitudinal study of the interrelationship between trabecular bone and articular cartilage in the osteoarthritic knee. Osteoarthritis Cartilage. 2004; 12:997–1005. [PubMed: 15564067]
35. Link TM, Steinbach LS, Ghosh S, Ries M, Lu Y, Lane N, et al. Osteoarthritis: MR imaging findings in different stages of disease and correlation with clinical findings. Radiology. 2003; 226:373–81. [PubMed: 12563128]
36. Majumdar S, Genant HK. Magnetic resonance imaging in osteoporosis. Eur J Radiol. 1995; 20:193–7. [PubMed: 8536747]
37. Majumdar S, Genant HK, Grampp S, Newitt DC, Truong VH, Lin JC, et al. Correlation of trabecular bone structure with age, bone mineral density, and osteoporotic status: in vivo studies in the distal radius using high resolution magnetic resonance imaging. J Bone Miner Res. 1997; 12:111–8. [PubMed: 9240733]
38. Majumdar S, Kothari M, Augat P, Newitt DC, Link TM, Lin JC, et al. High-resolution magnetic resonance imaging: three-dimensional trabecular bone architecture and biomechanical properties. Bone. 1998; 22:445–54. [PubMed: 9600777]
39. Majumdar S, Newitt D, Jergas M, Gies A, Chiu E, Osman D, et al. Evaluation of technical factors affecting the quantification of trabecular bone structure using magnetic resonance imaging. Bone. 1995; 17:417–30. [PubMed: 8573417]
40. Newitt DC, Majumdar S, van Rietbergen B, von Ingersleben G, Harris ST, Genant HK, et al. In vivo assessment of architecture and micro-finite element analysis derived indices of mechanical properties of trabecular bone in the radius. Osteoporosis International. 2002; 13:6–17. [PubMed: 11878456]
41. Eckstein F, Ateshian G, Burgkart R, Burstein D, Cicuttini F, Dardzinski B, et al. Proposal for a nomenclature for magnetic resonance imaging based measures of articular cartilage in osteoarthritis. Osteoarthritis and Cartilage. 2006; 14:974–83. [PubMed: 16730462]

42. McAlindon TE, Snow S, Cooper C, Dieppe PA. Radiographic patterns of osteoarthritis of the knee joint in the community: the importance of the patellofemoral joint. Annals of the Rheumatic Diseases. 1992; 51:844–9. [PubMed: 1632657]
43. Hayes CW, Jamadar DA, Welch GW, Jannausch ML, Lachance LL, Capul DC, et al. Osteoarthritis of the knee: comparison of MR imaging findings with radiographic severity measurements and pain in middle-aged women. Radiology. 2005; 237:998–1007. [PubMed: 16251398]
44. Yang NH, Nayeb-Hashemi H, Canavan PK, Vaziri A. Effect of frontal plane tibiofemoral angle on the stress and strain at the knee cartilage during the stance phase of gait. Journal of Orthopaedic Research. 2010; 28:1539–47. [PubMed: 20973057]
45. Mundermann A, Dyrby CO, D'Lima DD, Colwell CW Jr, Andriacchi TP. In vivo knee loading characteristics during activities of daily living as measured by an instrumented total knee replacement. Journal of Orthopaedic Research. 2008; 26:1167–72. [PubMed: 18404700]
46. Roemer FW, Khrad H, Hayashi D, Jara H, Ozonoff A, Fotinos-Hoyer AK, et al. Volumetric and semiquantitative assessment of MRI-detected subchondral bone marrow lesions in knee osteoarthritis: a comparison of contrast-enhanced and non-enhanced imaging. Osteoarthritis and Cartilage. 2010; 18:1062–6. [PubMed: 20472082]
47. Roemer FW, Frobell R, Hunter DJ, Crema MD, Fischer W, Bohndorf K, et al. MRI-detected subchondral bone marrow signal alterations of the knee joint: terminology, imaging appearance, relevance and radiological differential diagnosis. Osteoarthritis and Cartilage. 2009; 17:1115–31. [PubMed: 19358902]
48. Felson DT, Nevitt MC, Yang M, Clancy M, Niu J, Torner JC, et al. A new approach yields high rates of radiographic progression in knee osteoarthritis. Journal of Rheumatology. 2008; 35:2047–54. [PubMed: 18793000]
49. Burghardt AJ, Link TM, Majumdar S. High-resolution computed tomography for clinical imaging of bone microarchitecture. Clin Orthop Relat Res. 2011; 469:2179–93. [PubMed: 21344275]
50. Blumenfeld J, Studholme C, Carballido-Gamio J, Carpenter D, Link TM, Majumdar S. Three-dimensional image registration of MR proximal femur images for the analysis of trabecular bone parameters. Medical Physics. 2008; 35:4630–9. [PubMed: 18975709]
51. Kornaat PR, Kloppenburg M, Sharma R, Botha-Scheepers SA, Le Graverand MP, Coene LN, et al. Bone marrow edema-like lesions change in volume in the majority of patients with osteoarthritis; associations with clinical features. European Radiology. 2007; 17:3073–78. [PubMed: 17823802]
52. Stehling C, Lane NE, Nevitt MC, Lynch J, McCulloch CE, Link TM. Subjects with higher physical activity levels have more severe focal knee lesions diagnosed with 3T MRI: analysis of a non-symptomatic cohort of the osteoarthritis initiative. Osteoarthritis and Cartilage. 2010; 18:776–86. [PubMed: 20202488]

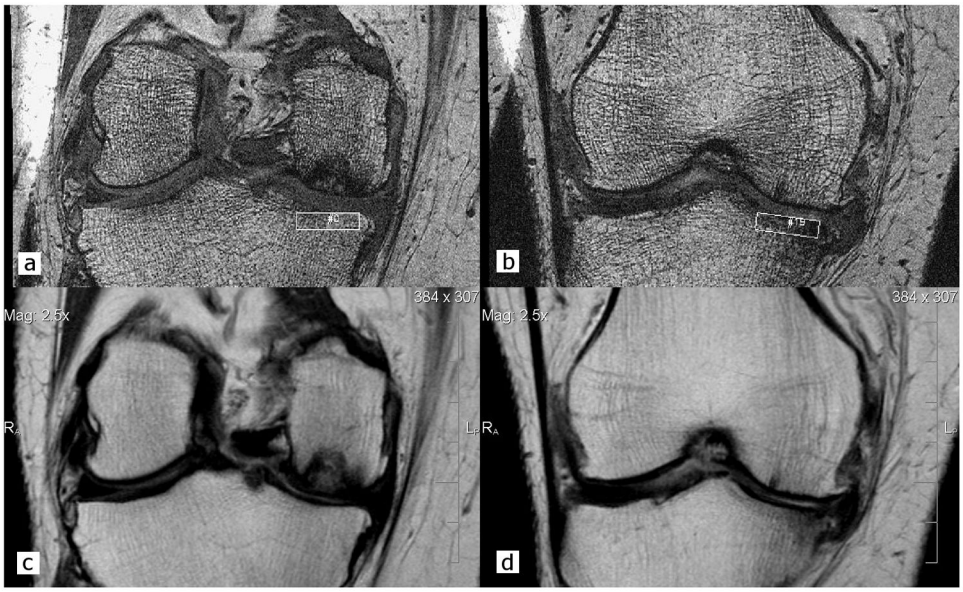

Figure 1.

Trabecular morphometry was quantified in the subchondral bone of the central medial proximal tibia using high-resolution coronal 3D FISP MR images with regions of interest (ROI; 3.75 mm [vertical] × 13.5 to 17.0 mm [medial-lateral]) located on 20 consecutive slices (a. most posterior image and b. most anterior image). c & d. To help localize the ROI and BMLs, coronal IW TSE images were registered to the trabecular images, to determine the corresponding slice range of interest (e.g., image a corresponds to image c and image b corresponds to image d).

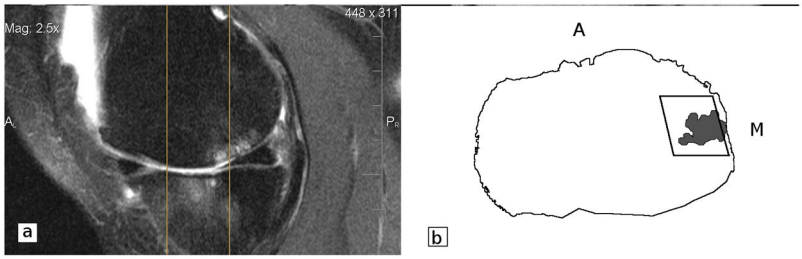

Figure 2.

a. Sagittal fat-suppressed IW TSE image were used to determine the presence, location and extent of the BML. Two vertical lines correspond to the locations of most anterior (Figure 1.c) and posterior (Figure 1.d) coronal slices. The reader identified anterior and posterior borders of the ROI and of the BMLs using the eFILM 3D Cursor tool. b. Pictorial representation of an axial image, with the ROI's width *medial-lateral] and depth [posterior-anterior] marked. Black line represents the outline of the proximal tibia. The grey irregular shape represents the bone marrow lesion. M = medial; A = anterior.

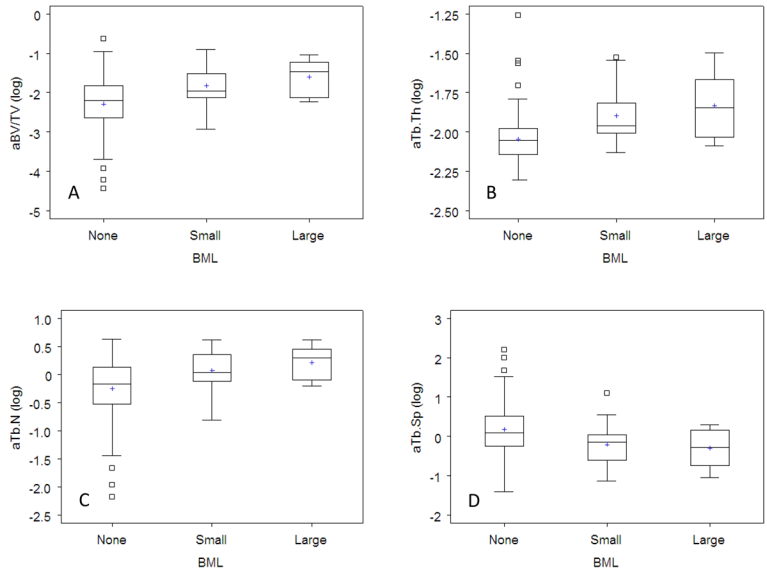

Figure 3.

Box plots demonstrating the distribution of trabecular measures (a. apparent bone volume fraction [aBV/TV], b. apparent trabecular thickness [aTB.Th], c. apparent trabecular number [aTB.N], d. apparent trabecular spacing [aTB.Sp]) in regions with no, small, or large bone marrow lesions (BMLs). The boxes represent the interquartile range of the trabecular measures and the whiskers demonstrate 1.5 times the interquartile range. Data beyond 1.5 times the interquartile range are indicated as small boxes. The horizontal line within the box represents the median while the plus sign defines the mean.

Table 1

Trabecular metrics (median, [min, max]) in regions with and without bone marrow lesions (BMLs) using Kruskal-Wallis tests

Relative BML size	Log Apparent Bone Volume Fraction	Log Apparent Trabecular Number (mm^{-1})	Log Apparent Trabecular Thickness (mm)	Log Apparent Trabecular Spacing (mm)
none (n=124)	−2.20 [−4.42, −0.62]	−0.17 [−2.17, 0.63]	−2.05 [−2.30, −1.26]	0.09 [−1.40, 2.22]
small (n=24)	−1.96 [−2.92, −0.90] *	0.03 [−0.81, 0.61] *	−1.96 [−2.13, −.52] *	−0.15 [−1.13, 1.10] *
large (n=10)	−1.46 [−2.23, −1.05] *	0.30 [−0.20, 0.61] *	−1.84 [−2.09, −1.50] *	−0.28 [−1.04, 0.30] *
Overall model p-value	p < 0.01	p < 0.01	p = 0.02	p < 0.01

* *p*-value of <0.05 for a pair-wise comparison with “none” as the referent group.